Field-stiffening effect of magneto-rheological elastomers

Yi Han [a], Wei Hong [a,*], LeAnn E. Faidley [b]

[a] Department of Aerospace Engineering, Iowa State University, Ames, IA 50011, USA
[b] Department of Chemistry and Engineering Science, Wartburg College, Waverly, IA 50677, USA

ARTICLE INFO

ABSTRACT

Magneto-rheological elastomers (MREs) are a class of soft active materials known for their tunable stiffness. Dispersed with magnetic particles, these polymer-based composites tend to be stiffer under a magnetic field. Such a stiffening effect is often attributed to the magnetic interaction among filler particles, but the well-acknowledged dipole-interaction model fails to explain the stiffening effect in tension/compression, which was observed in experiments. Other mechanisms, such as the effect of non-affine deformation, have been proposed, but there is no conclusive evidence on the dominating mechanism for the field-stiffening effect. This paper investigates various filler-chain structures, and seeks to identify the ultimate origin of the field-stiffening effect in MREs. Two different methods are used for cross verification: a dipole-interaction model and a finite-element simulation based on continuum field theories. This paper studies both the shear and axial deformation of the material, with a magnetic field applied in the particle-chain direction. It is found that while the magnetic interaction between particles is indeed the major cause of the stiffening effect, the wavy chain structure is the key to the modulus increase. Besides, chain–chain interaction and non-affine deformation are shown to be insignificant. In addition, the dependence of the stiffening effect on filler concentration is calculated, and the results qualitatively agree with experimental observations. The models also predict some interesting results that could be easily verified by future experiments.

© 2013 Elsevier Ltd. All rights reserved.

1. Introduction

Subject to a magnetic field, a magneto-active polymer may undergo a large deformation or change in its mechanical properties (e.g. stiffness). The capability of fast, reversible, and large deformation has made these materials promising candidates for next-generation actuators or artificial muscles (e.g. Faidley et al., 2010; Monz et al., 2008; Snyder et al., 2010; Zrínyi et al., 1997). The large field-induced volumetric strain of a porous magneto-active polymer may also be used in drug delivery (Zhao et al., 2011). The magneto-active polymers that exhibit a field-induced stiffening effect are known as magneto-rheological elastomers (MREs). Under an applied magnetic field, an MRE may significantly increase its shear modulus (e.g. Jolly et al., 1996; Shen et al., 2004; Zhou, 2003) and tensile modulus (e.g. Bellan and Bossis, 2002; Varga et al., 2006; Zhou, 2003). For brevity in description, we will refer to the field-stiffening effect as the magneto-rheological (MR) effect in this paper. The MR effect has endured MREs with numerous applications, such as smart vibration absorbers and damping components (e.g. Deng et al., 2006; Ginder et al., 2000; Hoang et al., 2011; Lerner and Cunefare, 2008), noise barrier system (Farshad and Roux, 2004), and sensors (e.g. Tian et al., 2011).

From a structural perspective, an MRE is a polymer-based composite filled with magnetic particles. While various polymers can been employed as the matrix material, silicon rubber and polyurethane are often used (e.g. Carlson and Jolly, 2000; Varga et al., 2006; Wu et al., 2010; Zajac et al., 2010). Due to their reliability and ease of manufacturing, micron-sized iron particles are usually used as the filler (e.g. Jolly et al., 1996; Rao et al., 2010; Zhou, 2003). The filler particles are usually dispersed during the curing process of the matrix elastomer, and their relative positions in the matrix are locked upon completion of the polymerization. In the absence of any external field, the filler particles are randomly distributed, and the resulting MREs have isotropic microstructure and magneto-mechanical properties. If an external magnetic field is applied at curing, the filler particles tend to align into chain-like structures, resulting in an MRE with highly anisotropic properties. Such anisotropic MREs have directional magnetic sensitivity, and exhibit a stronger MR effect than isotropic ones. Moreover, the MR effect is most significant when the applied magnetic field is in the direction along the particle-chains (e.g. Varga et al., 2006). All these evidences suggest a strong correlation between the MR effect and the microstructure of an MRE.

In past decades, constant efforts have been made in seeking the underlying mechanism of the MR effect. The simple and widely used model is based on the magnetic dipolar interaction between neighboring filler particles (Jolly et al., 1996). This model assumes

---

* Corresponding author. Tel.: +1 515 294 8850.
  E-mail address: whong@iastate.edu (W. Hong).

that all particles are magnetized in the same direction as the external magnetic field, and the particles are small enough to be considered as magnetic dipoles. Under such an assumption, the magnetostatic energy of the interaction between two neighboring dipoles is a function of the dipole moment m, the inter-particle distance r, and the angle between the line connecting the two dipoles and the direction of magnetization θ (Fig. 1a) (Rosensweig, 1985),

$$U = \frac{\mu_0 m^2}{4\pi r^3}(1 - 3\cos^2\theta),\tag{1}$$

where μ_0 is the vacuum permeability. As the interaction energy is proportional to r^{-3}, it attenuates quickly as the inter-particle distance increases, and thus an approximation can be made by accounting for the neighboring particles only. As sketched in Fig. 1a, when the material undergoes a shear γ, the angle θ changes from 0 to γ and the distance r increases as $r = r_0/\cos\gamma$. The change in the interaction energy contributes to the stress against the shear. The corresponding contribution to the shear stiffness,

$$\left.\frac{\partial^2 U}{\partial\gamma^2}\right|_{\gamma=0} = 3\frac{\mu_0 m^2}{\pi r_0^3},\tag{2}$$

is always positive. Consequently, the effective shear modulus increases with the applied field. This simple model has been widely used to explain the increase of the shear modulus of MREs under a magnetic field (e.g. Ivaneyko et al., 2011; Jolly et al., 1996). The model has been extended to account for the interactions among all particles of an infinitely long chain (Shen et al., 2004), as well as the interaction between parallel particle chains (Ivaneyko et al., 2011; Stolbov et al., 2011).

Although all these models recover the MR effect in shear, none of them is able to explain the MR effect in tension/compression. Subject to a normal strain ε along the chain direction, the inter-particle distance changes as $r = r_0(1 + \varepsilon)$, while the angle $\theta = 0$. Even though the dipolar contribution to the normal stress $\partial U/\partial\varepsilon > 0$, the contribution to the tensile stiffness,

$$\left.\frac{\partial^2 U}{\partial\varepsilon^2}\right|_{\varepsilon=0} = -3\frac{\mu_0 m^2}{\pi r_0^3},\tag{3}$$

is always negative. In contrast to the experimentally observed stiffening effect, this simple dipolar model results in a reduction in tensile modulus under an applied field. Similar conclusion has been obtained when iron particles form a rectangular-lattice microstructure (Ivaneyko et al., 2011).

We believe that the failure of this simple dipole-interaction model is mainly due to the incorrect microstructure assumed – the straight particle chains. In fact, available micrographs of MREs (e.g. Bobarth et al., 2012; Chen et al., 2007; Coquelle and Bossis, 2005) show that the particle-chains are often wavy rather than straight, as sketched in Fig. 1b. It has been suggested in the literature that wavy chains may explain the increased tensile modulus (Ivaneyko et al., 2011), but no rigorous theory or model has been proposed for this mechanism.

In addition to the dipolar interactions, other mechanisms have also been suggested for the MR effect, such as the local non-affine deformation of the polymer matrix. In a magnetic field, the neighboring particles in a chain of finite length may move closer to each other due to the magnetic attraction (e.g. Kankanala and Triantafyllidis, 2004), as sketched in Fig. 1c. As the particles are much stiffer than the matrix, the particle chain with narrower gaps would have a higher effective stiffness. Another type of non-affine deformation is the large distortion of the polymer matrix in between particle chains, as shown in Fig. 1c.

With all these mechanisms proposed but none verified, it becomes an urgent task to identify the ultimate origin of the MR effect in MREs. In the current paper, we seek to elucidate this puzzle by reconsidering all possible mechanisms. We will first calculate the MR effect from a wavy particle-chain structure by considering the dipolar interactions. Then we will compare the contributions from various mechanisms by computing the responses of a few representative unit cells with detailed microstructures using a finite-element method, in which both the polymer matrix and the filler particles are modeled as deformable continua, and the coupled magnetic and strain fields are solved simultaneously. Our calculations will show that the dominating mechanism for the MR effect is the magnetic dipolar interaction between particles forming wavy chains, while the contributions from chain–chain interaction and non-affine deformation are minor. This study also foresees the possibility of manufacturing a material with negative MR effect by placing the particles in straight chains.

2. Dipolar interaction in a wavy particle-chain

In this section, we will extend the simple dipole-interaction model (Jolly et al., 1996) by considering a wavy particle chain. Each magnetized filler particle is still treated as a magnetic dipole. The origin of the waviness in particle chains is quite natural. While the detailed chain structure depends on the complex curing pro-
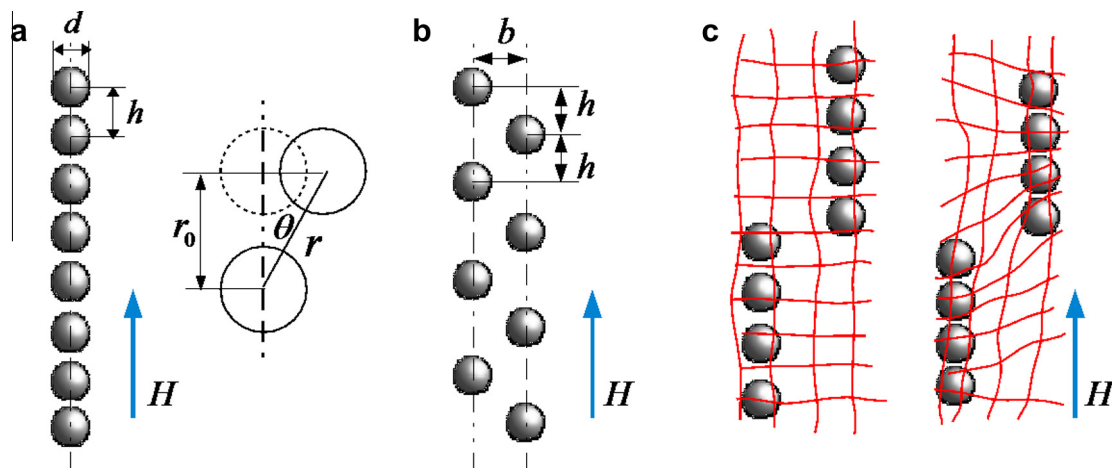

Fig. 1. Schematics of three possible mechanisms of the field-stiffening effect in an MRE: (a) dipolar interaction between particles in a straight chain, (b) dipolar interaction in a wavy particle chain, and (c) non-affine deformation of the polymer matrix. The geometric parameters are the particle diameter d, the horizontal distance b, and the vertical distance h between two neighboring particles.

cesses of MREs, such as the strength of the field applied, the initial dispersion, the viscosity of the polymer solution, and the speed of curing, basic physics suggests that a straight chain of aligned and equally spaced magnetic dipoles is unstable (Earnshaw, 1842). To enable analytical solution of the problem, we still assume the chain structure to be periodic and infinitely long, as sketched in Fig. 1b. The individual chains are assumed to be quite far from each other so that the interaction between chains is neglected. The structure is characterized by two geometric parameters: the horizontal distance b and vertical distance h between two neighboring particles. Particularly, a wavy chain reduces to a straight chain when $b = 0$.

Consider the case when the magnetic field is applied in the vertical direction, along the particle chains. When the material undergoes an elongation or compression along the same direction, the symmetry of the problem suggests that the dipole moment of each particle, $\mathbf{m}$, is also in the vertical direction. The magnetic interaction energy of per particle can be calculated by summing Eq. (1) over the contributions from all other particles:

$$U = \frac{\mu_0 m^2}{\pi h^3}[0.5f(\alpha) - 0.1503], \tag{4}$$

where $f(\alpha) = \sum_{n=1}^{\infty}(\alpha^2 - 2(2n-1)^2)(\alpha^2 + (2n-1)^2)^{-5/2}$, and $\alpha = b/h$ is a dimensionless geometry parameter representing the waviness of a chain. When $\alpha = 0$, the result reduces to that of a straight chain, $U \approx -1.2\mu_0 m^2/\pi h^3$.

The magnetic interaction energy per unit volume of the MRE can be written as $W_m = NU$, where N is the number of particles per unit volume. W_m changes with deformation. Let us first consider a uniaxial deformation along the chain direction, and assume that all particles undergo an affine deformation. The geometry of the chain structure varies accordingly with the axial stretch λ: h becomes λh, b becomes $\lambda^{-1}b$, and thus α becomes $\lambda^{-2}\alpha$. The magnetic energy density is thus also a function of the axial stretch λ,

$$W_m(\lambda) = \frac{N\mu_0 m^2}{\pi\lambda^3 h^3}\left[0.5f\left(\frac{\alpha}{\lambda^2}\right) - 0.1503\right]. \tag{5}$$

The magnetic energy gives rise to an additional stress $s_m = \partial W_m/\partial\lambda$, and an additional tensile modulus,

$$E_m = \left.\frac{\partial^2 W_m}{\partial\lambda^2}\right|_{\lambda=1}$$
$$= \frac{N\mu_0 m^2}{\pi h^3}\left[6f(\alpha) + 9\alpha f'(\alpha) + 2\alpha^2 f''(\alpha) - 1.8032\right]. \tag{6}$$

The normalized magnetic modulus, $\bar{E}_m = E_m\pi h^3/N\mu_0 m^2$, is plotted in Fig. 2. To show the fast attenuation of the magnetic interactions, we plot Eq. (6) together with the approximate result with only nearest neighbors considered. The small difference clearly shows the dominance of the interaction between neighboring particles. The results show that for relatively small α values (i.e. almost straight particle chains) the magnetic dipolar interaction has a negative contribution to the modulus. At the intermediate values of α (approximately 0.4–0.85, i.e. a relatively wavy chain), $\bar{E}_m$ is positive and maximizes at $\alpha \approx 0.6$. At large values of α, the chain under consideration is effectively divided into two parallel straight chains, and the magnetic contribution to the tensile modulus is also negative. The results at large values of α also indicate that the interaction between two straight chains could not give a positive MR effect in tension.

The prediction of this model is quite interesting. The MR effect is highly dependent on the particle alignment in each chain. Only an MRE containing wavy particle chains has positive MR effect in tension/compression. The fact that existing MREs mostly demonstrate positive MR effect indicates that most particle chains in these materials are wavy. If an MRE with relatively straight particle
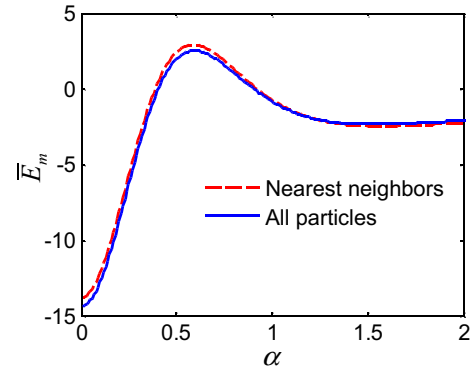

Fig. 2. Dimensionless contribution to the tensile modulus from magnetic dipole interactions, plotted as a function of the geometric parameter $\alpha = b/h$ (the waviness of a chain). Both the nearest-neighbor approximation (dash curve) and the result with interactions from all particles (solid curve) are presented.

chains could be manufactured, we expect that it would exhibit a negative MR effect, i.e. a reduction in tensile modulus under a magnetic field.

Using a similar approach, we also calculate the additional shear modulus induced by the magnetic dipolar interaction. Interestingly, the results are dependent on the relative direction of the shear deformation, as shown by Fig. 3. If the applied shear is perpendicular to the direction of the magnetic moments (case 1 on Fig. 3), the result is opposite to the tension case: a straight chain stiffens under a magnetic field but a wavy chain becomes more compliant. When the shear is parallel to the direction of the magnetic moments (case 2 on Fig. 3), the result is similar to the case of tension. One may argue that these two shear modes differ only by a rigid-body rotation, and case 1 is even closer to a usual experimental setup at first sight (e.g. Jolly et al., 1996; Shen et al., 2004; Zhou, 2003). However, it should be pointed out that, due to the presence of the dipole vectors, the difference between these two cases is more than just a rigid-body rotation. In fact, the physical difference lies on the magnetization behavior of the material. In case 1, the magnetic dipoles are always in the direction of the applied magnetic field, despite the shear-induced rotation of the particle chain. In case 2, the magnetic dipoles rotate together with the particle chain. Since the filler particles have much higher permeability than the polymer matrix, a particle chain creates a highly permeable
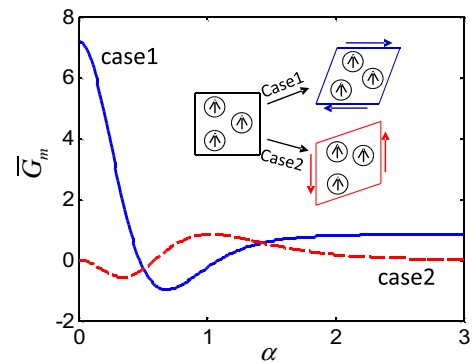

Fig. 3. Dimensionless contribution to shear modulus from magnetic dipole interactions, plotted as a function of the geometric parameter $\alpha = b/h$. The results depend on the relative direction of the shear-induced rotation and the direction of dipole moments. In the case when the dipoles stay in the original direction (case 1), a straight chain ($\alpha = 0$) has stiffening effect in shear, but a wavy chain of intermediate α values softens under a magnetic field. In the case when the dipoles follow the shear-induced rotation (case 2), a wavy chain shows stiffening effect at intermediate values of α.

pathway for the magnetic field in the composite, and consequently the magnetization would more likely follow the rotation caused by the shear deformation. Case 2, which gives a result closer to the experimental observations, may better represent the actual physical process. This speculation would be further validated by the numerical calculations in the following sections.

Although the dipolar interaction model provides a simple way of understanding the mechanism of the MR effect, and shows that a wavy-chain structure could explain the stiffening effect in both shear and tension/compression, it is still limited by the oversimplified model assumptions. First, the magnetic interactions between particles are modeled as that between dipoles. Such an approximation is valid when the inter-particle distance is much larger than the size of individual particles, whereas available micrographs showed that the gaps between particles are often comparable or even smaller than a particle (e.g. Bobarth et al., 2012; Chen et al., 2007). Second, the model assumes constant dipole moment for each filler particle, while in reality both the magnitude and the direction of magnetization would vary with deformation. Third, as discussed in the previous section, the presence of rigid particles may induce highly non-affine deformation, which may also affect the mechanical stiffness. To verify the prediction of this over-simplified model and to investigate the effects of other possible mechanisms, a different model which considers both filler particles and polymer matrix as continua will be introduced in Section 3 to study the stiffening effect via numerical simulations.

3. Material model and numerical calculation

The continuum theory of coupled magnetic field and mechanical deformation, namely the magneto-elasticity, has been well developed (e.g. Brigadnov and Dorfmann, 2003; Danas et al., 2012; Dorfmann and Ogden, 2004; Han et al., 2011; Kankanala and Triantafyllidis, 2004). The purpose of the current section is not to redevelop the theory, but to use it to study the field-stiffening mechanism of the composite material. We will thus omit the detailed derivation of the theory, and only list the governing equations and the specific material model. In contrast to homogenized models (e.g. Dorfmann and Ogden, 2004; Kankanala and Triantafyllidis, 2004; Ponte-Castañeda and Galipeau, 2011), we will study the effect of microstructures by considering the polymer matrix and the magnetic fillers as continua of distinct material properties.

Following the common approach of modeling deformable magnetic materials, we specify the material properties by introducing the Helmholtz free energy function W. Even though the composite exhibits a coupling behavior, neither the polymer matrix nor the filler particles have physically coupled magnetic and mechanical properties. Polymers are naturally non-magnetic, and the small magnetostriction of individual iron particles can be neglected. We therefore write the free energy into the sum of the magnetic contribution W_m and the elastic contribution W_s. For simplicity, we further assume the magnetic field is much lower than the saturation field, so that the materials can be modeled as linear magnetic, with magnetization energy density

$$W_m = \frac{B_i B_i}{2\mu}, \tag{7}$$

where μ is the permeability and B_i the magnetic induction. Repeated indices indicate a summation over all spatial dimensions. The elastic property is captured by the neo-Hookean model of free energy density

$$W_s = \frac{1}{2}G(F_{iK}F_{iK} - 3), \tag{8}$$

with G being the shear modulus, and F_{iK} the deformation gradient. An incompressible constraint, $\det F = 1$, is further prescribed by

using a Lagrange multiplier, p, i.e. the pressure field. To avoid introducing distributed mechanical moments and asymmetric true stress tensor, the field theory of magneto-elasticity is often written in terms of the nominal quantities measured with respect to the reference configuration. For example, the nominal magnetic induction $\widetilde{B}_K = B_i F_{Ki}^{-1}$, with F_{Ki}^{-1} being the inverse tensor components of the deformation gradient.

The specific form of free-energy function determines the constitutive relations. The nominal stress is related to deformation gradient and magnetic induction as

$$s_{iK} = \frac{\partial W}{\partial F_{iK}} = GF_{iK} + \frac{1}{\mu}\widetilde{B}_K \widetilde{B}_M F_{iM} - pF_{Ki}^{-1}, \tag{9}$$

and the nominal magnetic field

$$\widetilde{H}_K = \frac{\partial W}{\partial \widetilde{B}_K} = \frac{1}{\mu}\widetilde{B}_M F_{iM}F_{iK}. \tag{10}$$

In the absence of any body force, the mechanical equilibrium requires the divergence of the nominal stress to vanish

$$\frac{\partial s_{iK}}{\partial X_K} = 0. \tag{11}$$

Without any distributed current in the bulk, the static magnetic field satisfies Ampère's law,

$$\varepsilon_{iKM}\frac{\partial \widetilde{H}_M}{\partial X_K} = 0, \tag{12}$$

where ε_{iKM} is the permutation symbol. The spatial derivatives in the governing equations, (11) and (12), are both taken with respect to the material coordinates in the reference state.

The governing equations and the material model are implemented into a finite-element code (Han et al., 2011) using the commercial software COMSOL Multiphysics 4.2. As the detailed microstructure of an MRE is unknown, we are more interested in the dominating mechanism rather than the accurate prediction for one specimen. We thus implement the model in 2D, and calculate the representative unit cells in a material, such as the one sketched in Fig. 4b. In contrast to the dipole-interaction model, each filler particle is now modeled as a circular domain with diameter d. We assume the particles to be tightly bonded to the matrix, so that both displacement and traction are continuous across the interface. Different material properties are assigned to the filler and the matrix. Both the shear modulus and the magnetic permeability of the iron fillers are taken to be 1000 times higher than the corresponding parameters of the polymer matrix, $G_f/G_0 = \mu_f/\mu_0 = 10^3$, similar to those taken in the literature (Davis, 1999). To reduce the number of parameters, we normalize stresses by G_0, magnetic inductions by $\sqrt{\mu_0 G_0}$, and magnetic fields by $\sqrt{G_0/\mu_0}$. For a typical shear modulus of the polymer matrix, 1 MPa, a dimensionless magnetic field $H\sqrt{\mu_0/G_0} = 0.5$ is approximately 445 kA/m, which is far below the saturation field for iron particles (Carlson and Jolly, 2000). Thus the linear magnetic assumption in Eq. (7) should be valid.

Since the computational unit cells are much smaller than the size of a specimen, the boundary conditions are different from those on a macroscopic sample. Periodic boundary conditions are applied to the four sides of a unit cell, to represent a small piece of material in the middle of a large sample. To allow macroscopic deformation, the horizontal displacement on the right boundary has a constant but unknown offset, u_0, from that on the left boundary, $u_r = u_l + u_0$. Similar conditions are prescribed on the top and bottom boundaries, $v_t = v_b + v_0$.

The proper choice of magnetic boundary conditions is not obvious, as no magnetic field or electric current is applied directly on the boundaries of the unit cell. In experiments, magnetic fields
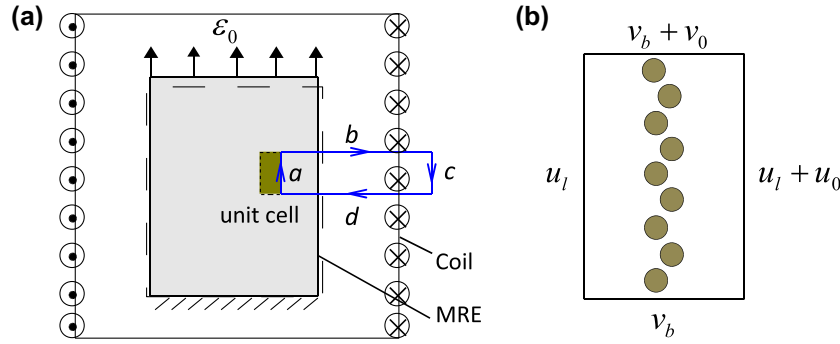
Fig. 4. (a) Sketch of an MRE with the magnetic field applied through an electromagnetic coil. (b) Sketch of a representative unit cell with a wavy chain. Periodic boundary conditions with constant offsets are applied on the displacements of all four edges of the unit cell.

have been applied in various ways to study the stiffening effect. In the tension or compression tests, magnetic fields are usually applied via electromagnetic coils where the MRE sample is placed at the center of the coil (e.g. Chertovich et al., 2010; Li et al., 2010; Varga et al., 2006), as sketched in Fig. 4a. Due to the different permeability of the sample and its surrounding air, the magnetic field is non-uniform. Let us neglect the surface effect by considering a small representative volume in the middle of the sample, in which the field is almost uniform. We thus apply periodical boundary conditions to the top and bottom edges of the unit cell, and symmetry boundary conditions to the left and right edges. The magnetic field is applied through an integral constraint. Consider the contour *a-b-c-d* on Fig. 4a, according to Ampère's law, the integration of the magnetic field along a closed contour equals the electric current it encloses. We may neglect the magnetic field outside the coil, and also that along the transverse sections (*b* and *d*) of the contour. Thus the true magnetic field along boundary *a* is related to the current density in the coil *J* as $\int_a H_t dl = Ja$, where H_t is the tangential component of the true magnetic field along the boundary. Since the coil rarely deforms with the sample, the true magnetic field *H* measured with respect to the current geometry keeps constant when the sample undergoes a tension or compression. To be consistent, we also evaluate the moduli by taking the derivatives of the true normal stress σ and shear stress τ with respect to the corresponding strains ε and γ, all measured in the current state. Therefore, in the following numerical examples, the MR effect is demonstrated by calculating the dependence of the tensile and shear moduli on the applied true magnetic field,

$$E(H) = \frac{\partial \sigma}{\partial \varepsilon}\bigg|_H \text{ and } G(H) = \frac{\partial \tau}{\partial \gamma}\bigg|_H \quad (13)$$

It should be mentioned that some experiments are done under approximately constant true magnetic induction by placing the sample between two permanent magnets, such as those measuring the MR effect in shear (Chen et al., 2007; Jolly et al., 1996; Kaleta and Lewandowski, 2007; Stepanov et al., 2007; Varga et al., 2006; Zajac et al., 2010). The measured constant-induction moduli, e.g. $\partial \tau/\partial \gamma|_B$, may differ from the constant-field moduli (13) in values, but should at least have the same sign and trend.

4. Results and discussion

First, the tensile moduli of unit cells with straight and wavy particle chains are studied. The chain structures are assumed to be infinitely long in both cases. In the numerical simulation, a 1% normal strain was applied to the unit cell along the chain direction. The tensile modulus $E(H)$ is evaluated from the finite-element output using Eq. (13). The results are normalized with the zero-field modulus $E(0)$, and plotted in Fig. 5 as a function of the dimension-

less field strength $H\sqrt{\mu_0/G_0}$, for various particle-chain geometries. Shown in Fig. 5a are the results of unit cells with straight particle chains ($\alpha = 0$) but different inter-particle distances ({h/d} = 1.1, 1.2, 1.3). Just like the prediction of the dipole-interaction model, the straight-chain structure has a negative MR effect (i.e. the field-induced stiffness decreases). Moreover, the relative change in the modulus decreases with h/d, as the composite is less permeable with large inter-particle distance, and thus the particles are less magnetized. As shown in Fig. 5b, the results with wavy particle chains are also consistent with the prediction of the dipole-interaction model. At intermediate values of α, wavy chain structures exhibit a positive MR effect in tension. Interestingly, the tensile modulus of some wavy chain structures (e.g. at $\alpha = 0.4$) is not a monotonic function of the applied field. At a relative high magnetic
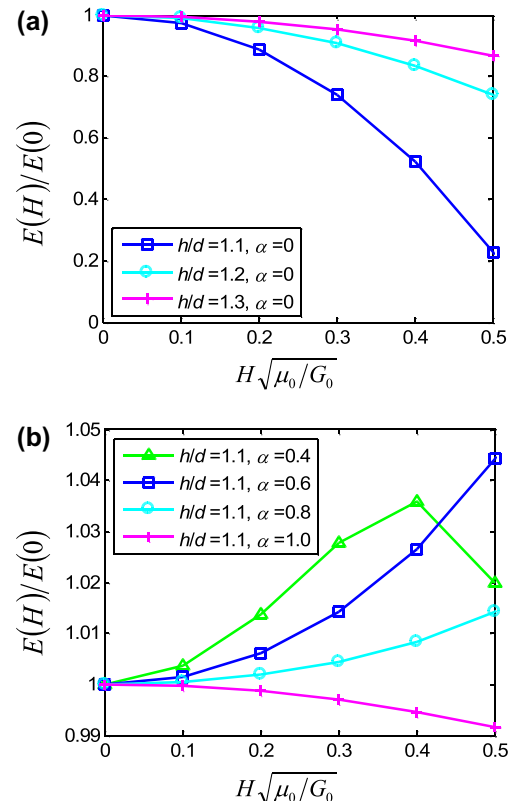

Fig. 5. Stiffening effect in the tensile modulus of MREs with different chain geometries: (a) straight chains ($\alpha = 0$) only give softening effect, which becomes weaker as the inter-particle distance increases; (b) wavy chains of intermediate α values have positive field-stiffening effect.
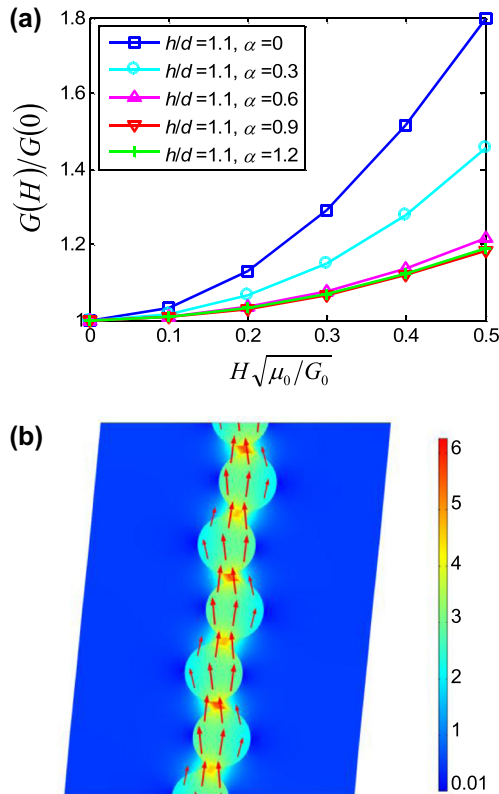
Fig. 6. (a) Stiffening effect in the shear modulus of MREs with different chain geometries: straight chains ($\alpha = 0$) give the strongest stiffening effect and wavy chains ($\alpha > 0$) also induce positive stiffening effect. (b) Rotation of a particle chain and the magnetization due to a shear deformation. The color scale shows the magnitude of the dimensionless true magnetic induction, and the arrows indicate the directions of the magnetization field.

field, the modulus decreases slightly. We believe that this phenomenon is caused by the local non-affine deformation. Under a strong magnetic field, the particles are aligned into straighter chains with smaller α.

The shear moduli $G(H)$ of these unit cells are also calculated and the results are plotted in Fig. 6, after normalization with the zero-field shear modulus $G(0)$. In contrast to the behaviors in tension,
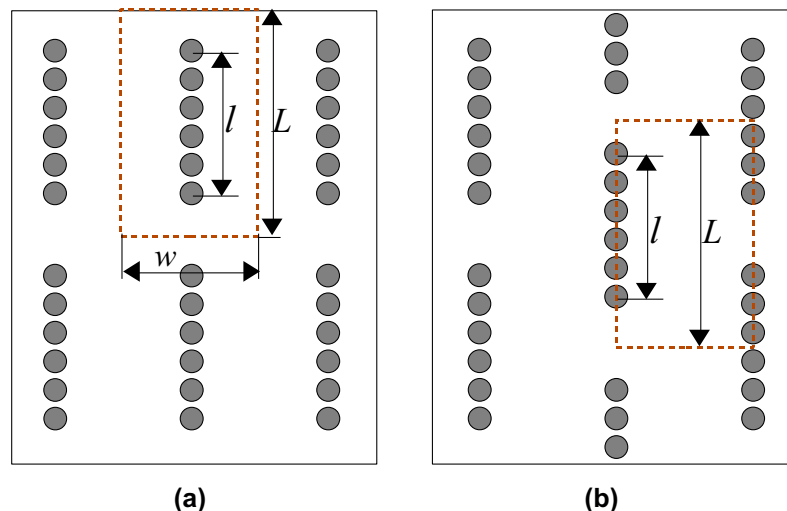
the particle-chain structures always exhibit a positive MR effect, and a straight chain ($\alpha = 0$) shows the highest relative change in the shear modulus. The results show that the behavior of particle chains is neither of the two ideal cases in the dipole-interaction model (Fig. 3). The magnetization of the iron particles neither remains in the direction of the external field, nor strictly follows the shear-induced rotation of the chains. As shown by Fig. 6b, the magnetization of the filler particles slightly rotates in the direction of shear, but the angle of rotation is smaller than the shear strain.

To further investigate the effect of deformation non-affinity in the particle-chain level, two more microstructures of MREs are studied. Instead of assuming the particle-chains to be infinitely long, we arrange finite particle chains side by side or staggered as shown by Fig. 7a and b, respectively, and select the computational unit cells as delineated by the dash lines. To focus on the contribution from non-affine deformation, we only consider the case of straight chains. Even though the two parallel chains may be regarded as an extreme case of one wavy chain, the separation corresponds to a large α value (>5) and is thus no different from two straight chains as suggested by the results shown in Figs. 2 and 3. The distance between neighboring particles within a chain is fixed at $h/d = 1.2$ and the aspect ratio of the unit cells is fixed at $w/L = 0.5$, where w and L are the width and length of the unit cells. The relative length of a particle chain l/L varies from 0.5 to 1. Under a 1% tensile strain, the deformation and the magnetic field are shown in Fig. 8. As expected, even under the low overall strain, both cases exhibit highly non-affine deformation: the inter-particle distance is significantly narrowed while the gaps between chains are extended. The local strain exceeds 20%. In addition, the staggered-chain structure shows a shear-lag pattern in the polymer matrix between two parallel chains with overlaps. The relative changes in tensile modulus of both types of structures are plotted in Fig. 9.

Despite the finite chain length and the staggered pattern, all results show a negative MR effect in tension. Although the structures with larger gaps (smaller l/L values) demonstrate a smaller decrease in the stiffness, we believe it is mainly caused by the decrease in the effective permeability of the structure – particle chains with larger gaps are less magnetized under the same field. This conclusion can be drawn by comparing between the behaviors of the side-by-side structure and the staggered structure. As shown by Fig. 9, the two types of structures are only slightly different in
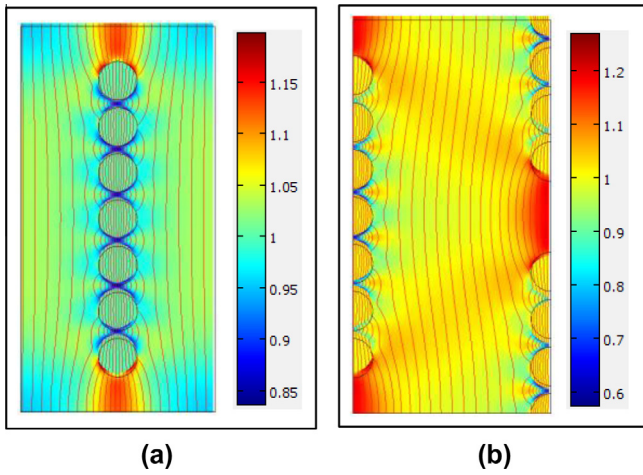

Fig. 7. Two representative microstructures of MREs containing particle chains of finite lengths: (a) chains are parallel and side by side, and (b) chains are staggered. The computational unit cells are marked by dash lines.

Fig. 8. Simulated non-affine deformation in unit cells under magnetic fields: the inter-particle distance is narrowed and the inter-chain gap is stretched. The magnetic induction field is shown by streamlines, and the vertical stretch is shown by color scale.
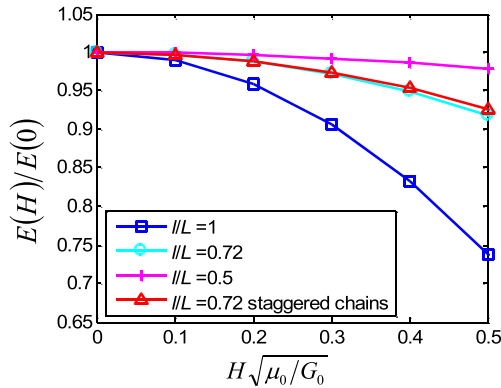

Fig. 9. Relative change in tensile modulus of MREs containing straight chains arranged side by side or staggered. All geometrics show a field-softening effect. The effect becomes weaker as the gap size increases.

Fig. 10. (a) Change of tensile modulus plotted as a function of the normalized true magnetic field, for MREs of various filler volume fractions. The numerical results fit well to a quadratic relation, $\Delta E \propto \mu_0 H^2$ (solid curves). (b) The dimensionless quantity $\Delta E/\mu_0 H^2$ from the fitting results, is approximately linear in filler volume fraction, ϕ.

terms of the stiffness change. The difference would be much more significant if the non-affine deformation were the dominating mechanism for the stiffness change, as the deformation patterns and load-carrying modes of the two structures are very different. We thus conclude that although the non-affine deformation under a magnetic field could cause stiffness increase, it plays a minor role compared to the effect of wavy chains in an anisotropic MRE. It may, however, explain the relatively low MR effect in isotropic MREs (Rao et al., 2010), in which particles are randomly distributed and no chain structure is present.

Finally, using the numerical model developed, we will study the effect of particle concentrations. It has been observed in experiments that MREs loaded with more iron particles usually have a stronger MR effect, both in shear and in tension/compression (Bellan and Bossis, 2002; Nikitin et al., 2006; Rao et al., 2010; Varga et al., 2006; Wu et al., 2011). For simplicity, only the structures of infinite long wavy chains with geometric parameter $\alpha = 0.6$ are considered. The volume fraction of filler particles, ϕ, is changed by tuning the width of the computational unit cells. The calculation results are presented in Fig. 10a. It is found that for each ϕ, the relation between the dimensionless change in tensile modulus $\Delta E/G_0$ and the dimensionless magnetic field $H\sqrt{\mu_0/G_0}$ fits well to a quadratic function, as shown by Fig. 10a. In other words, the absolute change in modulus scales with the square of the applied field, and
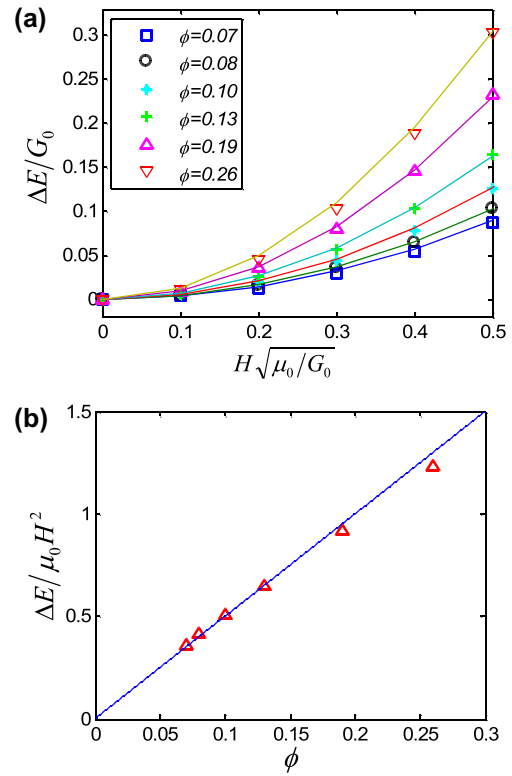
is independent of the elastic properties of the matrix. Such a result could be understood as a consequence of the dominance of the magnetic particle interactions over the non-affine deformation. This important result could be easily verified through experiments, e.g. by measuring the MR effect under different temperatures.

Subsequently, we fit all data in Fig. 10a by quadratic relations, and plot $\Delta E/\mu_0 H^2$, which represents the relative strength of the MR effect, as a function of the filler volume fraction in Fig. 10b. More interestingly, the dimensionless combination $\Delta E/\mu_0 H^2$ turns out to be almost linear in the filler volume fraction ϕ. Due to the limitation of the current 2D model and the coarse presentation of the microstructures, we are not confident on the accuracy of this linear relation, especially at high concentrations of filler particles. A densely loaded MRE could cause the particles to agglomerate and thus change the chain structure of the material. Nevertheless, the predicted trend that stronger MR effects are expected at higher filler concentrations is in agreement with experimental observations (e.g. Varga et al., 2006). A 3D finite element model with more realistic microstructures of MREs is expected to yield more accurate results, but is beyond the scope of this paper.

5. Concluding remarks

While the MR effect in magnetic-particle-filled polymer composites has been identified for decades, the dominating mechanism giving rise to this effect has never been identified clearly. It is clear though, that the mechanism is strongly correlated with the underlying microstructures of the materials. In this paper, we investigate the particle-chain structures of anisotropic MREs and identify the dominating mechanism that causes the MR effect using two methods. First, by modeling each particle as a magnetic dipole, we ana-

lytically derive the magnetic contribution to the stiffness of an MRE. The result shows that even though a straight chain could give MR effect in shear, the tensile modulus would decrease with magnetic field. On the other hand, a wavy chain could give rise to positive MR effect in both shear and tension/compression. To compensate the simplicity of the dipole-interaction model, we develop a finite-element model to simulate the behavior of material unit cells, which contain the polymer matrix and filler particles arranged into various patterns. Both the matrix and the fillers are modeled as continua of distinct material properties. The finite-element calculation confirms that the magnetic interaction among the filler particles in an MRE with wavy chains have positive MR effect in both shear and tension/compression. Furthermore, numerical calculations show that the contribution from non-affine deformation is present but insignificant, and would not yield a positive MR effect in MREs with straight chains.

Besides identifying the dominant mechanism of MR effect, our models have a few interesting predictions. It is shown analytically and numerically that an iron-particle-filled polymer composite would have a decrease in tensile stiffness under a magnetic field, if the particles are specially arranged to form straight chains. For a regular MRE, it is shown numerically that the stiffness increase scales with the square of the applied field, and is independent of the stiffness of the matrix material. The 2D numerical model also predicts an approximately linear dependence of the MR effect on the volume fraction of filler particles at relatively low filler concentrations. We are eagerly waiting for experimental verifications on the microstructural mechanism and on the predictions of the model.

Acknowledgments

References

Bellan, C., Bossis, G., 2002. Field dependence of viscoelastic properties of MR elastomers. Int. J. Modern. Phys. 16, 2447–2453.

Brigadnov, I.A., Dorfmann, A., 2003. Mathematical modeling of magneto-sensitive elastomers. Int. J. Solid. Struct. 40, 4659–4674.

Bobarth, T., Gunther, S., Borin, D.Yu., Gundermann, Th., Odenbach, S., 2012. XCT analysis of magnetic field-induced phase transitions in magnetorheological elastomers. Smart Mater. Struct. 21, 105018.

Carlson, J.D., Jolly, M.R., 2000. MR fluid, foam and elastomer devices. Mechatronics 10, 555–569.

Chen, L., Gong, X., Li, W., 2007. Microstructures and viscoelastic properties of anisotropic magnetorheological elastomers. Smart Mater. Struct. 16, 2645–2650.

Chertovich, A.V., Stepanov, G.V., Kramarenko, E.Y., Khokhlov, A.R., 2010. New composite elastomers with giant magnetic response. Macromol. Mater. Eng. 295, 336–341.

Coquelle, E., Bossis, G., 2005. Magnetostriction and piezoresistivity in elastomers filled with magnetic particles. J. Adv. Sci. 17, 132–138.

Danas, K., Kankanala, S.V., Triantafyllidis, N., 2012. Experiments and modeling of iron-particle-filled magnetorheological elastomers. J. Mech. Phys. Solids. 60, 120–138.

Davis, L.C., 1999. Model of magnetorheological elastomers. J. Appl. Phys. 85 (6), 3348–3351.

Deng, H., Gong, X., Wang, L., 2006. Development of an adaptive tuned vibration absorber with magnetorheological elastomer. Smart Mater. Struct. 15, N111–N116.

Dorfmann, A., Ogden, R.W., 2004. Nonlinear magnetoelastic deformations. Q. J. Mech. Appl. Math. 57, 599–562.

Earnshaw, S., 1842. On the nature of the molecular forces which regulate the constitution of the luminiferous ether. Trans. Camb. Philos. Soc. 7, 97–112.

Faidley, L.E., Han, Y., Hong, W., 2010. Axial strain of ferrogels under cyclic magnetic fields. Smart Mater. Struct. 19, 075001.

Farshad, M., Roux, M.L., 2004. A new active noise abatement barrier system. Polym. Testing 23, 855–860.

Ginder, J.M., Nichols, M.E., Elie, L.D., Clark, S.M., 2000. Controllable-stiffness components based on magnetorheological elastomers. Proc. Ser. SPIE Smart Struct. Mater. 3985, 418–425.

Han, Y., Hong, W., Faidley, L., 2011. Coupled magnetic field and viscoelasticity of ferrogel. Int. J. Appl. Mech. 3, 259–278.

Hoang, N., Zhang, N., Du, H., 2011. An adaptive tunable vibration absorber using a new magneto-rheological elastomer for vehicular powertrain transient vibration reduction. Smart Mater. Struct. 20, 015019.

Ivaneyko, D., Toshchevikov, V.P., Saphiannikova, M., Heinrich, G., 2011. Magneto-sensitive elastomers in a homogeneous magnetic field: a regular rectangular Lattice model. Macromol. Theory Simul. 20, 411–424.

Jolly, M.R., Carlson, J.D., Muñoz, B.C., 1996. A model of the behavior of magnetorheological materials. Smart. Mater. Struct. 5, 607–614.

Kaleta, J., Lewandowski, D., 2007. Inelastic properties of magnetorheological composites: I. Fabrication, experimental tests, cyclic shear properties. Smart Mater. Struct. 16, 1948–1953.

Kankanala, S.V., Triantafyllidis, N., 2004. On finely strained magnetorheological elastomers. J. Mech. Phys. Solids. 52, 2869–2908.

Lerner, A.A., Cunefare, K.A., 2008. Performance of MRE-based vibration absorbers. J. Intell. Mater. Syst. Struct. 19, 551–563.

Li, W., Zhou, Y., Tian, T., 2010. Viscoelastic properties of MR elastomers under harmonic loading. Rheol. Acta 49, 733–740.

Monz, S., Tschope, A., Birringer, R., 2008. Magnetic properties of isotropic and anisotropic CoFe2O4-based ferrogels and their application as torsional and rotational actuators. Phys. Rev. E 78, 021404.

Nikitin, L.V., Korolev, D.G., Stepanov, G.V., Mironova, L.S., 2006. Experimental study of magnetoelastics. J. Magn. Magn. Mater. 300, e234–238.

Ponte-Castañeda, P., Galipeau, E., 2011. Homogenization-based constitutive models for magnetorheological elastomers at finite strain. J. Mech. Phys. Solids 59, 194–215.

Rao, P.V., Maniprakash, S., Srinivasan, S.M., Srinivasa, A.R., 2010. Functional behavior of isotropic magnetorheological gels. Smart Mater. Struct. 19, 085019.

Rosensweig, R.E., 1985. Ferrohydrodynamics. Cambridge University Press.

Shen, Y., Golnaraghi, M.F., Heppler, G.R., 2004. Experimental research and modeling of magneto-rheological elastomers. J. Intell. Mater. Syst. Struct. 15, 27.

Snyder, R.L., Nguyen, V.Q., Ramanujan, R.V., 2010. Design parameters for magneto-elastic soft actuators. Smart Mater. Struct. 19, 055017.

Stepanov, G.V., Abramchuk, S.S., Grishin, D.A., Nikitin, L.V., Kramarenko, E.Y., Khokhlov, A.R., 2007. Effect of a homogeneous magnetic field on the viscoelastic behavior of magnetic elastomers. Polymer 48, 488–495.

Stolbov, O.V., Raikher, Y.L., Balasoiu, M., 2011. Modeling of magnetodipolar striction in soft magnetic elastomers. Soft Matter 7, 8484–8487.

Tian, T., Li, W., Deng, Y., 2011. Sensing capabilities of graphite based MR elastomers. Smart Mater. Struct. 20, 025022.

Varga, Z., Filipcsei, G., Zrínyi, M., 2006. Magnetic field sensitive functional elastomers with tunable elastic modulus. Polymer 47, 227–233.

Wu, J., Gong, X., Fan, Y., Xia, H., 2010. Anisotropic polyurethane magnetorheological elastomer prepared through in situ polycondensation under a magnetic field. Smart Mater. Struct. 19, 105007.

Wu, J., Gong, X., Fan, Y., Xia, H., 2011. Physically crosslinked poly(vinyl alcohol) hydrogels with magnetic field controlled modulus. Soft Matter 7, 6205.

Zajac, P., Kaleta, J., Lewandowski, D., Gasperowicz, A., 2010. Isotropic magnetorheological elastomers with thermoplastic matrices: structure, damping properties and testing. Smart Mater. Struct. 19, 045014.

Zhou, G., 2003. Shear properties of a magnetorheological elastomer. Smart Mater. Struct. 12, 139–146.

Zhao, X., Kim, J., Cezar, C., Huebsch, N., Lee, K., Bouhadir, K., Mooney, D., 2011. Active scaffolds for on-demand drug and cell delivery. Proc. Nat. Acad. Sci. 108, 67.

Zrínyi, M., Barsi, L., Szabó, D., 1997. Direct observation of abrupt shape transition in ferrogels induced by nonuniform magnetic field. J. Chem. Phys. 106 (13), 5682–5692.